JOURNAL OF SOLID STATE CHEMISTRY **131,** 2–8 (1997)
ARTICLE NO. SC967240

Vibrational Analysis of $Ba_{5-x}Sr_xNb_4O_{15}$ Microwave Dielectric Ceramic Resonators

R. Ratheesh, H. Sreemoolanadhan, and M. T. Sebastian[1]

Regional Research Laboratory, Industrial Estate, Trivandrum 695 019, India

Received August 5, 1996; in revised form September 18, 1996; accepted November 20, 1996

The $Ba_{5-x}Sr_xNb_4O_{15}$ ceramics have been prepared and characterised using XRD, Raman, FTIR, and microwave dielectric property measurements. The measured dielectric properties show smooth variation with Sr content. The spectroscopic studies show that the symmetry of the NbO_6 octahedra increases with increase in strontium content, maintaining the hexagonal structure. Hence, the possibility of a monoclinic structure for $Sr_5Nb_4O_{15}$ seems to be inappropriate. The observed symmetric stretching bands of NbO_6 octahedra confirm the existence of corner connected octahedra in all the solid solution compounds. The behavior of the dielectric constant of $(Ba_{5-x}Sr_x)Nb_4O_{15}$ system can be correlated to the variation of symmetric stretching vibrations of NbO_6 octahedra. © 1997 Academic Press

INTRODUCTION

The perovskite-type materials possess excellent properties that make them potentially useful for catalytic, electronic, and ion exchange applications (1). The crystal structure of a series of perovskite-type materials $R_5M_4O_{15}$ (R = Ba, Sr; M = Nb, Ta) have been studied by Galasso and Katz (2, 3). They reported that $Ba_5Nb_4O_{15}$ has a hexagonal structure (space group $P\bar{3}m1$) with one molecular unit per crystallographic unit cell, whereas the strontium analogue could not be formed or more generally nontypical from other members of the group (2). The polytypism of $Ba_5Nb_4O_{15}$ has been studied by Hutchinson *et al.* (4, 5). Later, Whiston and Smith (6) prepared and characterized the $Sr_5Nb_4O_{15}$ material and reported the crystal structure as hexagonal. However, Weiden *et al.* (7) reported the crystal structure of $Sr_5Nb_4O_{15}$ material as monoclinic (space group $P2/m$) with two molecular units per crystallographic unit cell. Recently, it was found (8, 9) that ceramics in the BaO–SrO–Nb_2O_5 system possess excellent dielectric properties that make them suitable for applications in communication systems. In order to clarify the ambiguities that exist in the structural studies, we have performed Raman and infrared spectroscopic investigation of these materials.

EXPERIMENTAL

The $(Ba_{5-x}Sr_x)Nb_4O_{15}$ $\{x = 0$ corresponds to *B*5N4, $x = 1$ to *B*4S, $x = 2$ to *B*3S2, $x = 3$ to *B*2S3, $x = 4$ to *B*S4, and $x = 5$ to S5N4$\}$ ceramics were prepared by the conventional solid state route. Starting materials were high purity $BaCO_3$, $SrCO_3$, and Nb_2O_5. The stoichiometric mixtures, after wet mixing, were calcined in the range 1250–1375 °C for 4 h depending on the strontium content (x). These powders were thoroughly ground and were then sintered at 1400–1450°C for 4 h. Sintered compacts had a diameter of 9–10 mm and a thickness of 5–6 mm. All of the compositions showed densification except S5N4 which did not densify even after firing at 1600°. However, addition of 1 wt% of Y_2O_3 after calcination is found to be very effective in densifying S5N4. XRD patterns were taken using powder samples. Raman spectra were recorded using both a Dilor Z24 triple monochromator and a Spex 1401 double monochromator equipped with a Spectra Physics model 165.08 argon ion laser with an experimental resolution better than 3 cm^{-1}. The infrared spectra were recorded on a Brucker IFS 66V infrared spectrometer with samples in the 50–400 cm^{-1} region taken as polyethylene and 400–4000 cm^{-1} using KBr pellets.

The dielectric constant (ε_r) and unloaded quality factor of the ceramics in the microwave frequency region were measured using an HP 8510 B Network Analyzer coupled with accessories and controlled by an HP 9000, 300 computer. The dielectric constant was obtained from the TE_{011} mode under the end-shorted condition (10). For the determination of the unloaded quality factor (Q_u) the stripline method proposed by Khanna and Garault (11) was used. The ceramics were coupled to a microstripline in a brass enclosure. The unloaded quality factors were found from the response

[1] To whom correspondence should be addressed. E-mail: mts@csrrltrd.ren.nic.in.

0022-4596/97 $25.00

of the band rejection filters. For the coefficient of temperature variation of frequency (τ_f) an HP 8410 C Network Analyzer and an HP 8350 B sweep oscillator were used. The shift of the $TE_{01\delta}$ mode of the resonators, placed centrally at the bottom of an aluminium cavity, was determined in the temperature range 25–80°C.

FACTOR GROUP ANALYSIS

$Ba_5Nb_4O_{15}$ crystallizes (2) in the hexagonal system with space group $P\bar{3}m1$ having one formula unit per Bravais cell. The crystal structure of $Ba_5Nb_4O_{15}$ is analogous to $Ba_5Ta_4O_{15}$ (2) and can be described as a five-layer repeat closest packing of oxygen with a barium replacing one oxygen in each layer in the unit cell (see Fig. 1). As in $Ba_5Ta_4O_{15}$, the niobium ions in $Ba_5Nb_4O_{15}$ are in octahedral coordination with oxygen and the octahedra share corners, except for the third and fourth layers of oxygen, which are not shared. The niobium ions are located in the octahedral holes between layers. However, there are five such holes and only four niobium ions so that one niobium ion is missing between one pair of layers.

The factor group analysis has been carried out on the basis of correlation method developed by Fateley *et al.* (12) to get the irreducible representations. The 72 normal modes of vibrations of the title compound, at $k = 0$ under D_{3d} factor group splits into

$$\Gamma B5N4 = 5\,A_{1g} + 3\,A_{2g} + 4\,A_{1u} + 12\,A_{2u} + 8\,E_g + 16\,E_u.$$

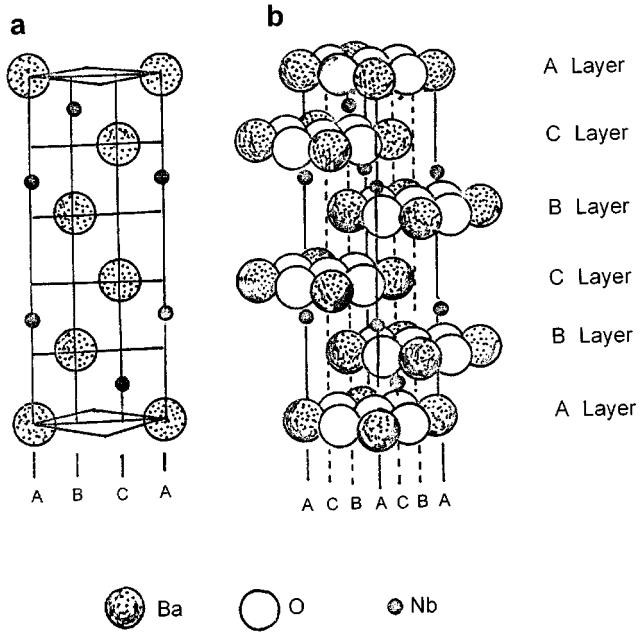

FIG. 1. Crystal structure of $Ba_5Nb_4O_{15}$ showing the layer arrangement of ions (From Ref. 3).

If S5N4 is isostructural with that of *B*5N4 one can expect 72 normal modes of vibrations. According to Weiden *et al.* (7), S5N4 has a monoclinic distortion which leads to a unit cell with symmetry $P2/m$ with twice the volume of the hexagonal cell. The structure consists of a closest packing of five Sr–O layers with the niobium ions located in corner-sharing octahedral holes. So the 144 normal modes of vibrations of S5N4 under C_{2h} factor group at $k = 0$, splits into

$$\Gamma S5N4 = 36\,A_g + 36\,B_g + 36\,A_u + 36\,B_u.$$

RESULTS AND DISCUSSION

The microwave dielectric properties $(Ba_{5-x}Sr_x)Nb_4O_{15}$ ceramics are given in Table 1. It is evident from the table that the ε_r of these ceramics increases with Sr content up to $x = 3$ and then decreases. But the change in ε_r below $x = 3$ is found to be small. The variation of ε_r of $(Ba_{5-x}Sr_x)Nb_4O_{15}$ ceramics with respect to Sr content (x) is shown in Fig. 2.

The powder X-ray diffraction patterns of $(Ba_{5-x}Sr_x)Nb_4O_{15}$ ceramics obtained using Cu$K\alpha$ radiation are shown in Fig. 3. XRD patterns of these samples are very similar, excluding some weak reflections which show the isostructural nature of these ceramics. The pattern of $Ba_5Nb_4O_{15}$ is in agreement with the earlier report (JCPDS No. 14-28). The pattern of $Sr_5Nb_4O_{15}$ shows additional weak reflections, which may be due to the secondary phases as observed by Whiston and Smith (6). The patterns are indexed based on hexagonal symmetry. The lattice parameters a, c, and (c/a) ratio as well as bulk densities are calculated and are given in Table 1. The calculated lattice parameters of $Ba_5Nb_4O_{15}$ and $Sr_5Nb_4O_{15}$ match with those reported earlier (2, 6). Figure 4 shows the variation of a, c and (c/a) as a function of x. The (c/a) ratio increases up to $x = 2$ and then decreases. The change in a below $x = 3$ is very small. The smooth curve of c shows a maximum near $x = 3$. The smooth nature of variations of the lattice parameters and the measured dielectric properties with Sr substitution suggest a possible direct relationship.

But in the structural analysis of $Sr_5Nb_4O_{15}$, Weiden *et al.* suggests that this compound has a monoclinic structure with twice the volume of the hexagonal cell. To verify the crystal structure of $Sr_5Nb_4O_{15}$, and to understand the changes taking place in the structure of $Ba_5Nb_4O_{15}$ due to progressive substitution of strontium, we have carried out a systematic vibrational analysis of all the solid solution ceramics.

VIBRATIONAL ANALYSIS

The NbO_6 octahedron with O_h symmetry has six fundamental vibrations (13–15), namely symmetric stretching mode ν_1 (A_{1g}), asymmetric stretching modes ν_2 (E_g), and ν_3

TABLE 1
Lattice Parameters and Microwave Dielectric Properties of $Ba_{5-x}Sr_xNb_4O_{15}$ Ceramics

Material	Lattice parameters		(c/a) ratio	ε_r	$Q \times f$ ($\times 10^{12}$)	Bulk density (g/cc)
	a (Å)	c (Å)				
$Ba_5Nb_4O_{15}$	5.79	11.75	2.029	38.4	12.7	6.07
$Ba_4SrNb_4O_{15}$	5.77	11.78	2.042	48.4	9.8	5.64
$Ba_3Sr_2Nb_4O_{15}$	5.76	11.81	2.050	49.5	16.5	5.44
$Ba_2Sr_3Nb_4O_{15}$	5.75	11.76	2.045	50.6	21.2	5.41
$BaSr_4Nb_4O_{15}$	5.65	11.51	2.037	44.9	44.0	5.46
$Sr_5Nb_4O_{15}$	5.63	11.40	2.025	39.7	6.6	5.20

(F_{1u}), asymmetric bending mode v_4 (F_{1u}), symmetric bending mode v_5 (F_{2g}), and the inactive mode v_6 (F_{2u}). The group theoretical considerations represent 15 internal modes of an NbO_6 octahedron as $A_{1g} + E_g + 2F_{1u} + F_{2g} + F_{2u}$. Among them A_{1g}, E_g, and F_{2g} are Raman active, the two F_{1u} modes are IR active, whereas F_{2u} is inactive in both. However, the deviation from O_h symmetry will result in line broadening or even splitting. Complete removal of symmetry will result in 15 bands. Since Nb^{5+} is too small to form regular NbO_6 octahedra, in most of the oxide systems it looses its O_h symmetry due to distortions (16). Depending on the extent of distortion, NbO_6 octahedra can have (17) five different symmetries, viz. D_{4h}, D_{3d}, C_{4v}, C_{3v}, and C_{2v}.

In the Raman spectrum of *B*5N4, five bands are observed in the nondegenerate symmetric stretching region (1, 18) of the NbO_6 octahedra (Table 2). Out of the five bands observed (Fig. 5(a)), the one at 785 cm^{-1} is of very strong intensity. The corresponding infrared spectrum gives two bands in this region (Fig. 6a). In the Raman spectrum of *B*5N4, large splitting is observed for the symmetric stretching region. The extent of splitting shows that these bands are not arising due to the considerable coupling of the modes amongst the octahedra (19, 20). The presence of different

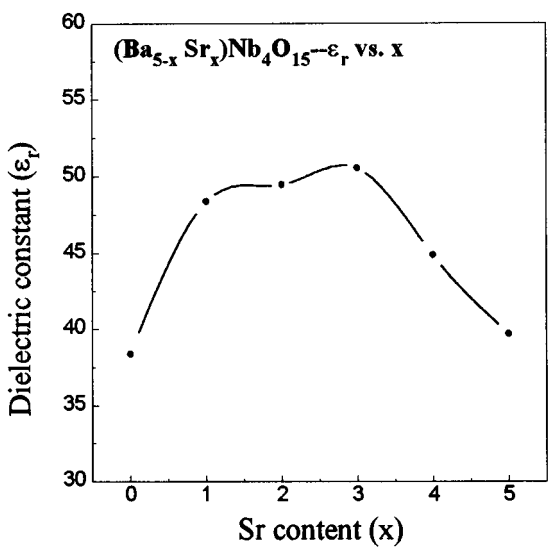

FIG. 2. Variation of ε_r of $(Ba_{5-x}Sr_x)Nb_4O_{15}$ ceramics with respect to Sr content (x).

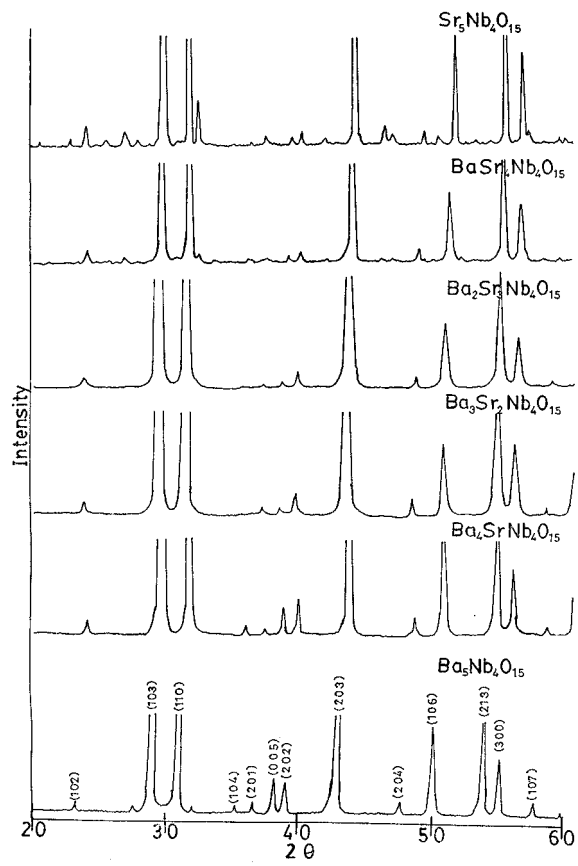

FIG. 3. Powder XRD patterns of $(Ba_{5-x}Sr_x)Nb_4O_{15}$ ceramics obtained using Cu$K\alpha$ radiation.

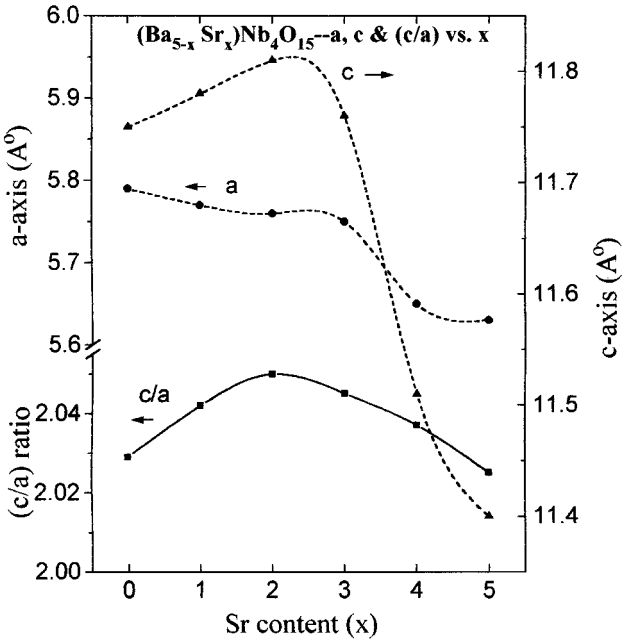

FIG. 4. Variation of lattice parameters of $(Ba_{5-x}Sr_x)Nb_4O_{15}$ ceramics with respect to Sr content (x).

Nb–O bond lengths may be the reason for such a large splitting of this nondegenerate mode in *B*5N4.

When the strontium concentration is increased, the number of split components of the ν_s Nb–O modes is reduced considerably. This shows that the distortion of NbO_6 octahedra is reduced as a result of Sr substitution. We can see a gradual shifting of the strongest symmetric stretching vibrations of the NbO_6 octahedra toward the higher wavenumber regions. For *B*4S, the strongest ν_s Nb–O band is observed at 790 cm^{-1}, whereas for *B*3S2, it is shifted to 806 cm^{-1}. The shift of this mode is maximum for *B*2S3, where the NbO_6 octahedra give rise to a very strong band at 823 cm^{-1}. Further increase of Sr substitution decreases the stretching vibrations to lower wavenumber regions (see Fig. 5b and 5c). The variation of symmetric stretching vibration of NbO_6 octahedra with respect to x is shown in Fig. 7. The variation is similar to that observed in the case of the ε_r (Fig. 2). From the observed spectral changes, it can be inferred that in $Ba_5Nb_4O_{15}$, NbO_6 octahedra are tightly packed compared to Sr-substituted compositions and have different Nb–O bond lengths. With the increase in the strontium concentration, NbO_6 octahedra become regular since the c parameter increases though the ionic radius of Sr

TABLE 2
Spectral Data and Band Assignments of $(Ba_{5-x}Sr_x)Nb_4O_{15}$ Ceramics

$x = 0$ (*B*5N4)		$x = 1$ (*B*4S)		$x = 2$ (*B*3S2)		$x = 3$ (*B*2S3)		$x = 4$ (*B*S4)		$x = 5$ (S5N4)		
Raman	IR	Raman	IR	Raman	IR	Raman	IR	Raman	IR	Raman	IR	Assignments
898 w 851 m 796 s 785 vs 742 sh	852 m 807 mbr	844 mbr 790 vs	852 m 804 mbr	854 mbr 806 vsbr		823 vs	835 m	806 vs	833 m	803 vs	831 m	ν_1 NbO_6
683 wbr	704 vsbr	679 m	702 vsbr	689 w		693 w	708 vsbr	677 wbr	709 vsbr	676 w	698 vsbr	ν_2 NbO_6
548 mbr 510 vw	565 vsbr 507 m	551 mbr	560 vsbr 507 m	569 m		583 m	600 vsbr	574 m	586 vsbr	582 mbr	589 vsbr	ν_3 NbO_6
448 m 441 m	430 w	439 m	429 m	453 m	431 m	457 mbr	429 s	438 mbr	428 m	445 m 389 vw	427 m	ν_4 NbO_6
389 vvw 320 s	391 mbr	305 s	391 mbr	322 s		344 m 327 s	398- 252 sbr	325 s 315 s	396- 209 sbr	341 s 328 m	396- 206 sbr	ν_5 NbO_6
	294 sbr		294 sbr		298 sbr					281 w		ν_6 NbO_6
277 vw 170 m 129 vvs 107 w 93 vw	265 s 225 m 164 m 144 m 110 m 75 m 58 w	237 w 159 m 116 vvs	259 mbr 228 m 155 wbr 141 m 110 m 75 m 57 m	251 wbr 176 m 131 vvs 115 w 93 w	230 m 154 m 140 m 113 w 79 w	255 wbr 180 mbr 138 vvs 99 m 91 vw	232 sbr 138 mbr 117 mbr 81 m	238 wbr 174 w 125 s 103 w 91 w 60 w 38 m	157 mbr 143 m 116 w 83 m	262 w 251 w 189 w 163 w 136 s 119 w 106 w 72 vw	163 mbr 149 mbr 119 w 90 m	Lattice modes

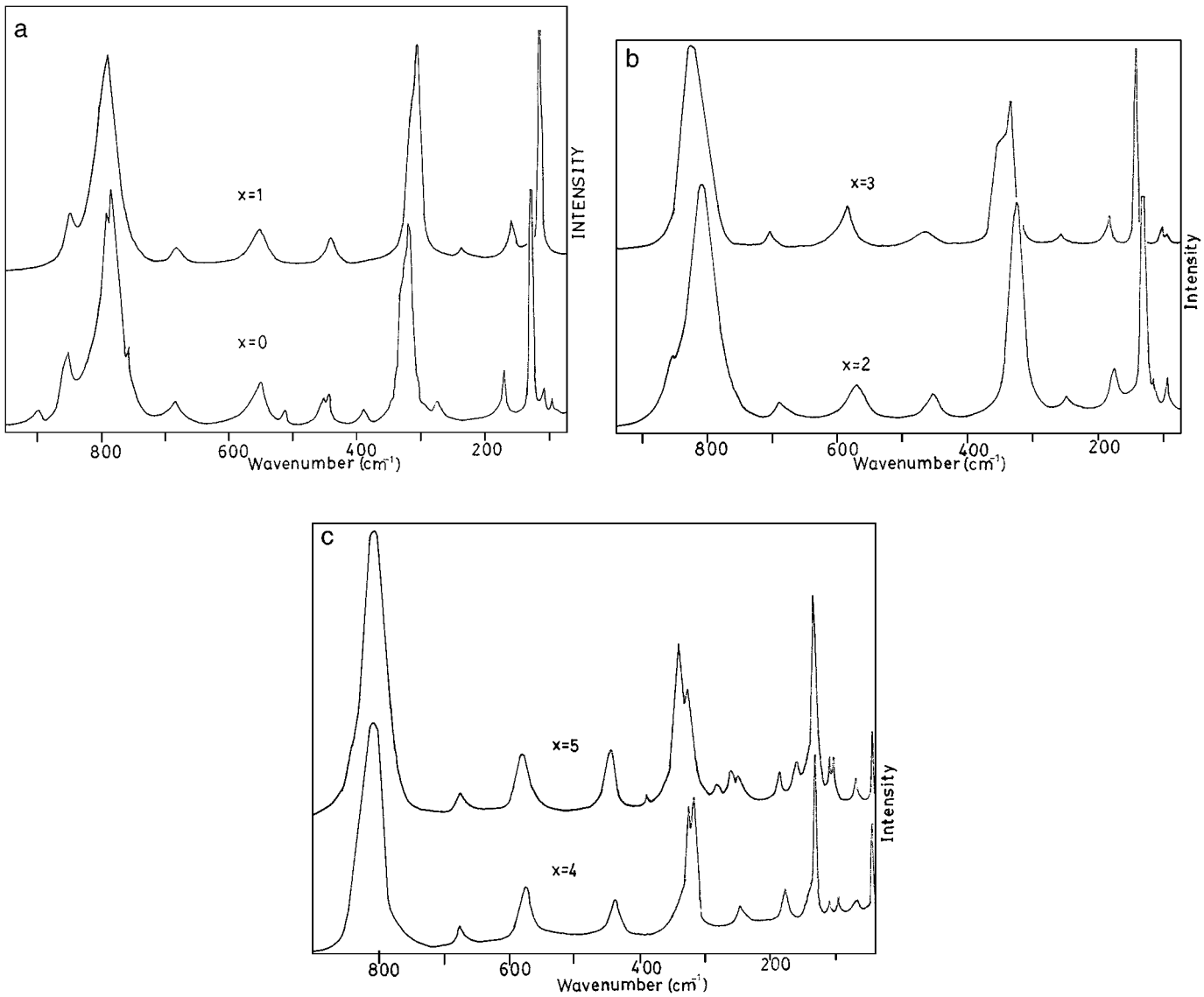

FIG. 5. (a) Raman spectra of $Ba_5Nb_4O_{15}$ and $(Ba_4Sr)Nb_4O_{15}$ ceramics. (b) Raman spectra of $(Ba_3Sr_2)Nb_4O_{15}$ and $(Ba_2Sr_3)Nb_4O_{15}$ ceramics. (c) Raman spectra of $(BaSr_4)Nb_4O_{15}$ and $Sr_5Nb_4O_{15}$ ceramics.

(1.40 Å) is less than that of Ba (1.60 Å). This is evident from the disappearance of the split components in the Sr-rich composition. Accordingly, the NbO_6 octahedra as a whole must be rotated about their three axes, shifting the strongest symmetric stretching vibrations toward the higher wavenumber regions. Since the distortion of the NbO_6 octahedra decreases with Sr substitution, the dielectric behavior of these ceramics may be attributed to the rotation of the NbO_6 octahedra.

Generally, corner-shared and edge-shared octahedra are predominant in niobium–oxygen polyhedra. Edge-shared octahedra exhibit large distortions than do corner-shared octahedra, resulting in significant variations in Nb–O bond lengths. For edge-shared octahedra, the Nb–O bond length varies from 1.7 to 2.3 Å, whereas in corner-connected octahedra Nb–O bond lengths are in the range 1.9 to 2.0 Å (2, 21). From the structural studies it is evident that NbO_6 octahedra in $Ba_5Nb_4O_{15}$ are corner-connected (2, 3). In the case of an edge-shared NbO_6 octahedra the symmetric stretching vibrations are usually observed in the 850–1000 cm^{-1} region, whereas in corner-connected octahedra these vibrations are observed in the 750–850 cm^{-1} region (2, 22, 23). In the present study, symmetric stretching vibrations support the existence of corner-connected NbO_6 octahedra in all of these compositions (Table 2) as reported by Galasso and Katz.

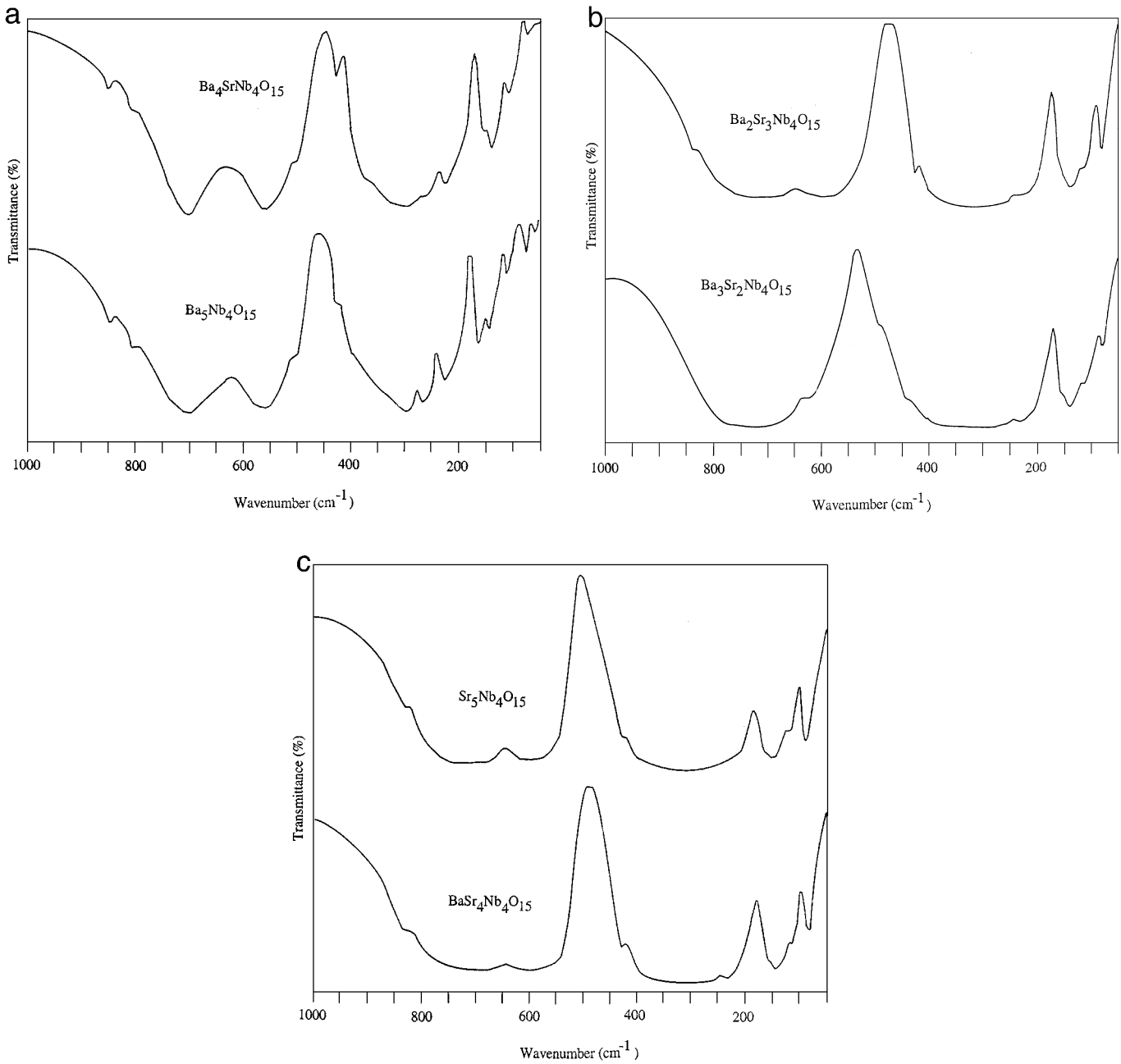

FIG. 6. (a) FTIR spectra of $Ba_5Nb_4O_{15}$ and $(Ba_4Sr)Nb_4O_{15}$ ceramics. (b) FTIR spectra of $(Ba_3Sr_2)Nb_4O_{15}$ and $(Ba_2Sr_3)Nb_4O_{15}$ ceramics. (c) FTIR spectra of $(BaSr_4)Nb_4O_{15}$ and $Sr_5Nb_4O_{15}$ ceramics.

Raman bands due to v_2 (E_g), mode of a perfect NbO_6 octahedra are weak since Nb^{5+} ion with the d^0 configuration participates significantly in π bonding (2, 25). However the extensive distortion of NbO_6 octahedra give rise to higher intensity v_2 bands. Even though IR inactive, very strong bands are observed in the infrared spectrum of all the studied materials compared to relatively weak Raman bands in this region.

As expected, very strong bands are observed in the IR active v_3 (F_{1u}) mode of the NbO_6 octahedra in these solid solutions (Fig. 6). Observing fewer bands in the symmetric and asymmetric bending (v_5 and v_4) mode regions (Table 2) suggests the retention of degeneracy of the NbO_6 octahedra in these compositions. The bands observed around 295 cm^{-1} in the infrared spectra of most of these compositions may be due to the inactive v_6 (F_{2u}) mode (15).

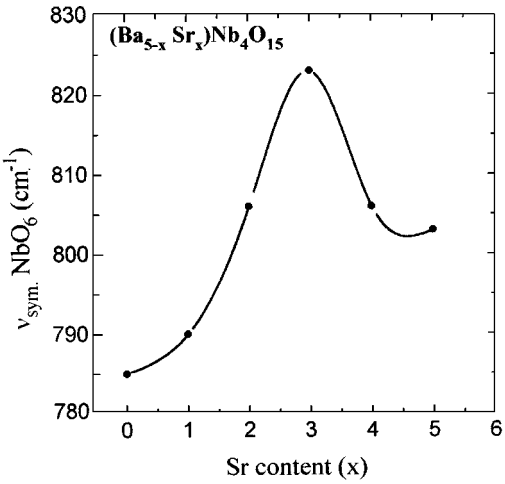

FIG. 7. Variation of strongest symmetric stretching vibration of NbO_6 octahedra with respect to x.

The bands observed below 280 cm^{-1} are due to lattice modes. An unambiguous assignment of these modes is not possible since this region consists of vibrations due to translational and rotational modes of NbO_6 octahedra and metal–oxygen stretching modes. However, it is worth noting that as the strontium concentration increases, more bands are observed in the lattice mode region. The maximum number of modes appear in $Sr_5Nb_4O_{15}$ in this region (Fig. 5c). The extra bands appearing in this region in the Raman spectra of strontium-rich compositions can be attributed to the secondary phases (6).

If the $Sr_5Nb_4O_{15}$ compound possessed a monoclinic structure with two formula units per crystallographic unit cell, as reported by Weiden *et al.* (7), more bands should have been observed corresponding to the symmetric stretching vibrations (26) of the NbO_6 octahedra (see factor group analysis). Sugiyamma and Nagai (27) observed additional splitting for the strontium-rich composition (monoclinic) the $(Ba_{1-x}Sr_x)(Mg_{1/3}Ta_{2/3})O_3$ system, due to the reduction in symmetry compared to the barium rich one (hexagonal). Thus, it follows from the vibrational analysis of the $(Ba_{5-x}Sr_x)Nb_4O_{15}$ ceramics, that the symmetry of the NbO_6 octahedra is increasing with strontium substitution keeping the crystal system unchanged. Hence, it can be concluded that the $Sr_5Nb_4O_{15}$ has a hexagonal structure in accordance with the report of Whiston and Smith.

ACKNOWLEDGMENTS

R. Ratheesh and H. Sreemoolanadhan are grateful to CSIR, New Delhi for research fellowships. The authors are grateful to Dr. P. Mohanan for microwave measurements.

REFERENCES

1. G. T. Stranford and R. A. Condrate Sr., *J. Mater. Sci. Lett.* **3,** 303 (1984).
2. F. Galasso and L. Katz, *Acta Crystallogr.* **14,** 647 (1961).
3. F. S. Galasso, *Structure and Properties of Inorganic Solids*, Pergamon, Elmsford, NY, 1970.
4. J. L. Hutchinson and A. J. Jacobson, *Acta Crystallogr. B* **31,** 1442 (1975).
5. J. L. Hutchinson, *Chem. Scripta* **14,** 181 (1978–79).
6. C. D. Whiston and A. J. Smith, *Acta Crystallogr.* **23,** 82 (1967).
7. M. Weiden, A. Grauel, J. Norwig, S. Horn, and F. Steglich, *J. Alloys Compounds* **218,** 13 (1995).
8. H. Sreemoolanadhan, M. T. Sebastian, and P. Mohanan, *Mater. Res. Bull.* **30**(6), 653 (1995).
9. C. Vineis, P. K. Davies, T. Negas, and S. Bell, *Mater. Res. Bull.* **31**(5), 431 (1996).
10. W. E. Courtney, *IEEE Trans. Microwave Theory Tech.* **18**(8), 476 (1970).
11. A. P. S. Khanna and Y. Garault, *IEEE Trans. Microwave Theory Tech.* **31**(3), 261 (1983).
12. W. G. Fateley, F. R. Dollish, N. T. Mc Devitt, and F. F. Bentley, *Infrared and Raman Selection Rules for Molecular and Lattice Vibrations—The Correlation Method*, Wiley, New York, 1972.
13. G. M. Clark and W.P. Doyle, *Spectrochim Acta* **22,** 141 (1966).
14. M. Liegeois-Duyckaerts and P. Tarte *Spectrochim. Acta. A* **30,** 1771 (1974).
15. R. Ratheesh, G. Suresh, and V. U. Nayar, *J. Solid. State Chem.* **118,** 351 (1995).
16. L. E. Orgel, *An Introduction to Transition Metal Chemistry*, p. 134, Wiley, New York, 1960.
17. A. Ann McConnell, J. S. Anderson, and C. N. R. Rao, *Spectrochim. Acta A* **32,** 1067 (1976).
18. G. Blasse and A. F. Corsnit, *J. Solid State Chem.* **6,** 513 (1973).
19. T. S. N. Moorthy, V. Srinivas, G. Saibabu, and M. Salagram, *J. Solid State Chem.* **97,** 358 (1992).
20. D. Philip and G. Aruldhas, *J. Raman Spectrosc.* **21,** 211 (1990).
21. G. Blasse and G. P. M. Van Den Heuvel, *J. Solid State Chem.* **10,** 206 (1974).
22. A. El Jazouli, C. Parent, J. M. Dance, G. Le Flem, P. Hagenmuller, and J. C. Viala, *J. Solid State Chem.* **74,** 377 (1988).
23. U. Balachandran and N. G. Eror, *J. Mater. Sci. Lett.* **1,** 374 (1982).
24. G. Blasse, *J. Inorg. Nucl. Chem.* **26,** 1191 (1964).
25. J. B. Goodenough and J. A. Kafalas, *J. Solid State Chem.* **6,** 493 (1973).
26. R. Zurmuhlen, E. Colla, D. C. Dube, J. Petzelt, I. Reaney, A. Bell, and N. Setter, *J. Appl. Phys.* **76**(10), 5864 (1994).
27. M. Sugiyamma and T. Nagai, *Jpn. J. Appl. Phys.* **32,** 4360 (1993).